Electrophysiological identification of daily rhythms in the prefrontal cortex

Brandon L. Roberts[1], Jiexin Wang[1] and Ilia N. Karatsoreos[1]

[1] Neuroscience and Behavior Program, and Department of Psychological and Brain Sciences, University of Massachusetts Amherst, Amherst, MA 01003, USA

Running Head: Daily rhythms in PFC

Correspondence should be sent to:

Ilia N. Karatsoreos, Ph.D.

Department of Psychological and Brain Sciences

University of Massachusetts Amherst

Tobin Hall, 135 Hicks Way

Amherst, MA 01003

E-mail: ikaratsoreos@umass.edu

Word count: Abstract (199), Introduction (756), Results (1,436), Discussion (2,237), Methods (1,027)

Figures: (6)

Figure supplements: (2)

Figure data files: (7)

Abstract

Circadian rhythms are ubiquitous in biology, from the molecular to behavioral levels. There is growing interest in understanding the functional implications of circadian oscillations in different cells and systems, including the brain. The prefrontal cortex (PFC) is heavily involved in myriad processes, including working memory, cognition, stress responses, and fear associated behaviors. Many PFC associated behaviors are time-of-day dependent, yet how time-of-day impacts the basic function of neurons in the PFC is not known. Here we use patch-clamp electrophysiology to record from layer 2/3 pyramidal neurons in the prelimbic (pl) PFC of male and female C57BL/6J mice at 4 separate bins of zeitgeber time (ZT): 0-4, 6-10, 12-16, and 18-22. We measured changes in membrane properties, inhibitory and excitatory inputs, ion channel function, and action potential kinetics. We demonstrate that the activity of plPFC neurons, their inhibitory inputs, and action potential dynamics are regulated by time-of-day. Further, we show that in males postsynaptic K^+ channels play a central role in mediating these rhythms, suggesting the potential for an intrinsic gating mechanism mediating information throughput. These key discoveries in PFC physiology demonstrate the importance of understanding how daily rhythms contribute to the mechanisms underlying the basic functions of PFC circuitry.

Introduction

Rhythms in life are found at many different time scales in nearly all phyla. From annual rhythms in hibernation and reproduction, to daily rhythms in sleep-wake cycles, to ultradian rhythms such as variations in heart rate, to rhythms in coordinated brain activity (Helm et al. 2013; Körtner and Geiser 2000; Yaniv and Lakatta 2015; M. H. Hastings, Reddy, and Maywood 2003). They are also present at nearly all levels of organization, from the behavior of groups of organisms to gene and protein expression at the cellular level (Jagannath et al. 2017; Landgraf et al. 2016; J. W. Hastings 2007). Given their ubiquity in nature and involvement in countless biological processes, understanding the functional significance of these rhythms is critical. However, while major strides have been made in understanding how these rhythms impact cellular function in the suprachiasmatic nucleus (SCN), as well as in some peripheral organs such as the liver, there remains a paucity of information about the functional impact of circadian clocks in other brain regions, beyond identifying that circadian rhythms are present (Abe et al. 2002; Albrecht and Stork 2017; Sato et al. 2020; Weaver 1998). This is a major gap in our knowledge, considering that circadian rhythms in behaviors are well documented, and shown to be critical in both health and disease.

The PFC serves as a critical component in cognition, emotional systems involved in fear learning and extinction, stress responses, and learning and memory, all of which are impacted by daily rhythms (Woodruff et al. 2018; McCarthy and Welsh 2012; Popoli et al. 2012; Sotres-Bayon, Cain, and LeDoux 2006; Miller and Cohen 2001). In addition, clock gene expression has been documented in the prefrontal cortex (PFC) (Chun et al. 2015). The prelimbic area (pl) of the PFC is divided into six distinct layers, each with distinct inputs and projections. Specifically, layer 2/3 plays a major role in working memory and behavioral plasticity and is involved in stress and depressive behaviors (Yuen et al. 2009; Zaitsev et al. 2012; Radnikow and Feldmeyer 2018; Moorman et al. 2015). The PFC is comprised of a wide array of cell types, including excitatory pyramidal neurons, which impact behavior by relaying information to other brain regions that are under clear circadian control, such as the amygdala and hippocampus, and inhibitory interneurons, such as the parvalbumin (PV+) and neuropeptide Y (NPY) containing neurons (Kawaguchi and Kubota 1997; Radnikow and Feldmeyer 2018; Vertes 2006; Saffari

et al. 2016). On whole, the function, synaptic inputs and intrinsic physiological characterizations of these neurons are heterogeneous throughout the PFC.

plPFC pyramidal neurons receive excitatory glutamatergic and inhibitory GABAergic presynaptic input, with findings suggesting these are differentially regulated in male and female mice (Popoli et al. 2012; Saffari et al. 2016; Andrade et al. 2012; de Velasco et al. 2015; Pena-Bravo et al. 2019). Excitatory inputs onto these neurons are plastic and environmental factors such as stress, learning and memory, can lead to long-lasting potentiation of glutamatergic inputs onto these neurons through increased NMDAR and AMPAR mediated currents (Yuen et al. 2009; Laroche, Jay, and Thierry 1990). Over activation of plPFC neurons is detrimental to normal behavioral function, and inhibitory inputs, which arise from the numerous inhibitory interneurons throughout the PFC, serve to mitigate the excitability of PFC neurons (Ferguson and Gao 2018). The majority of PFC pyramidal neurons are intrinsically quiescent at rest and regulate information throughput via a wide array of ion channels, including cyclic-nucleotide-gate non-selective cation (HCN) channels, and calcium (Ca^{2+}) and potassium (K^{+}) channels known to mediate postsynaptic throughput of excitatory and inhibitory currents (Kalmbach and Brager 2020; Zaitsev et al. 2012; Deng et al. 2019; Workman et al. 2015). In the SCN, changes in sodium (Na^{+}), K^{+}, and Ca^{2+} ion channel function mediate daily rhythms in the spontaneous activity, and action potential dynamics of neurons (Bano-Otalora et al. 2021). How these channels might impact daily rhythms in PFC function and the gating of information throughput is unknown.

Given the importance of understanding how daily rhythms impact PFC function, and our previously documented effects of circadian desynchronization on PFC structure (Karatsoreos et al. 2011), here we rigorously tested how time-of-day alters a wide range of neurophysiological properties in plPFC pyramidal neurons. The data presented here thoroughly demonstrate that time-of-day clearly impacts the basal activity of these neurons. Second, we show that inhibitory and excitatory synaptic inputs fluctuate throughout the day in a sex dependent manner. Lastly, we identify that K^{+} channels may serve, in part, as a mechanism to regulate daily changes in information throughput in plPFC pyramidal neurons.

Results

Resting membrane potential of prelimbic layer 2/3 pyramidal neurons is rhythmic in male mice.

The regional and cell specific heterogeneity in electrophysiological properties of PFC pyramidal neurons has been described in multiple species (Zaitsev et al. 2012; van Aerde and Feldmeyer 2015; Piette et al. 2021). Layer 2/3 pyramidal neurons of the plPFC were identified visually by anatomical location (**Figure 1A;** *left*). Pyramidal neurons were identified by shape and lucifer yellow (LY; 0.2%) was added to the patch pipette for confirmation of an apical dendrite (**Figure 1A;** *right*).

To test our hypothesis that time-of-day impacts the basal electrophysiological properties of pyramidal neurons, we performed whole-cell patch clamp techniques and measured RMP, membrane capacitance (Cm), and membrane resistance (Rm) at ZT bins: 0-4, 6-10, 12-16, and 18-22 in male and female mice (**Figure 1B-E**). For RMP there was a main effect of time (no effect of sex) and interestingly, within group post-hoc analysis revealed that plPFC pyramidal neurons in male mice are more depolarized at ZT6-10 (light period), when compared to 12-16 and 18-22 (dark period). Post-hoc analysis did not reveal a time-of-day effect on RMP in female mice (**Figure 1C**). We did not observe an interaction between sex and time in any of our measures; however, there was a main effect of sex on Rm (**Figure 1E**). Together, these data demonstrate that the RMP of plPFC pyramidal neurons in male mice changes throughout the light/dark (LD) cycle.

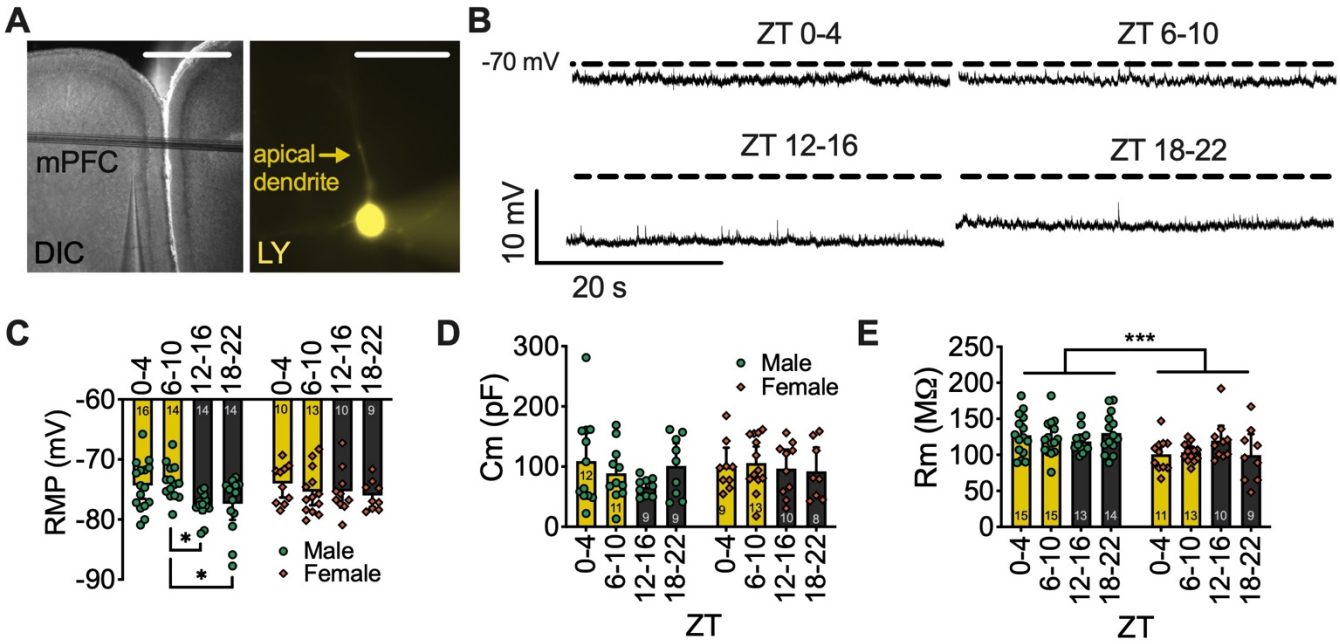

Figure 1. *Time-of-day changes in membrane potential of layer 2/3 mPFC pyramidal neurons.* **(A)** Image of mPFC slice (*left;* scale 1mM) and layer 2/3 pyramidal neuron backfilled with lucifer yellow (LY, *right;* scale 10 μM). **(B)** Representative traces of current clamp recordings from male mice at each ZT bin. **(C)** Mean and individual data points for membrane potential (RMP) at ZT0-4, 6-10, 12-16, and 18-22 in male (*bluish green circles*) and female (*vermillian diamonds*) mice **(D)** Mean membrane capacitance (Cm) and **(E)** resistance (Rm) binned by ZT. Error bars represent ± 95% CI. N-values for number of cells inset on bars. Two-way ANOVA for main effects and interaction with a within group Tukey post-hoc analysis for ZT bin, * $p < 0.05$, ***$p < 0.001$. Exact p-values, mouse N-values, and analysis in **Figure 1 – source data 1**.

sEPSC activity on plPFC pyramidal neurons is time-of-day dependent

Glutamatergic pyramidal neurons are the predominant cell-type in the plPFC, project to extra-PFC cortical, subcortical and limbic regions, and interconnect within the PFC (Le Merre, Ährlund-Richter, and Carlén 2021). We hypothesized that basal excitatory glutamatergic release contributes to daily changes in RMP and predicted that the number and/or strength of excitatory inputs are highest during the light period, when plPFC pyramidal neurons are depolarized (**Figure 1B, C**). To test whether time-of-day alters excitatory inputs we used the whole-cell voltage-clamp configuration (V_H = -70mV) to record sEPSCs in plPFC pyramidal neurons from male and female mice at ZT0-4, 6-10, 12-16, and 18-22 (**Figure 2A-E**). There was a main effect of ZT time on sEPSC frequency, but not amplitude, and post-hoc analysis demonstrated that in male mice the frequency of excitatory inputs was increased during the dark period, when RMP is hyperpolarized, an effect counter to our hypothesis (**Figure 1B and 2A-C**). Further, we observed clear sex differences on both sEPSC frequency and amplitude (**Figure 2D, E**). These data suggest that time-of-day impacts the number of excitatory inputs (frequency), but not their strength (amplitude) in male and female mice.

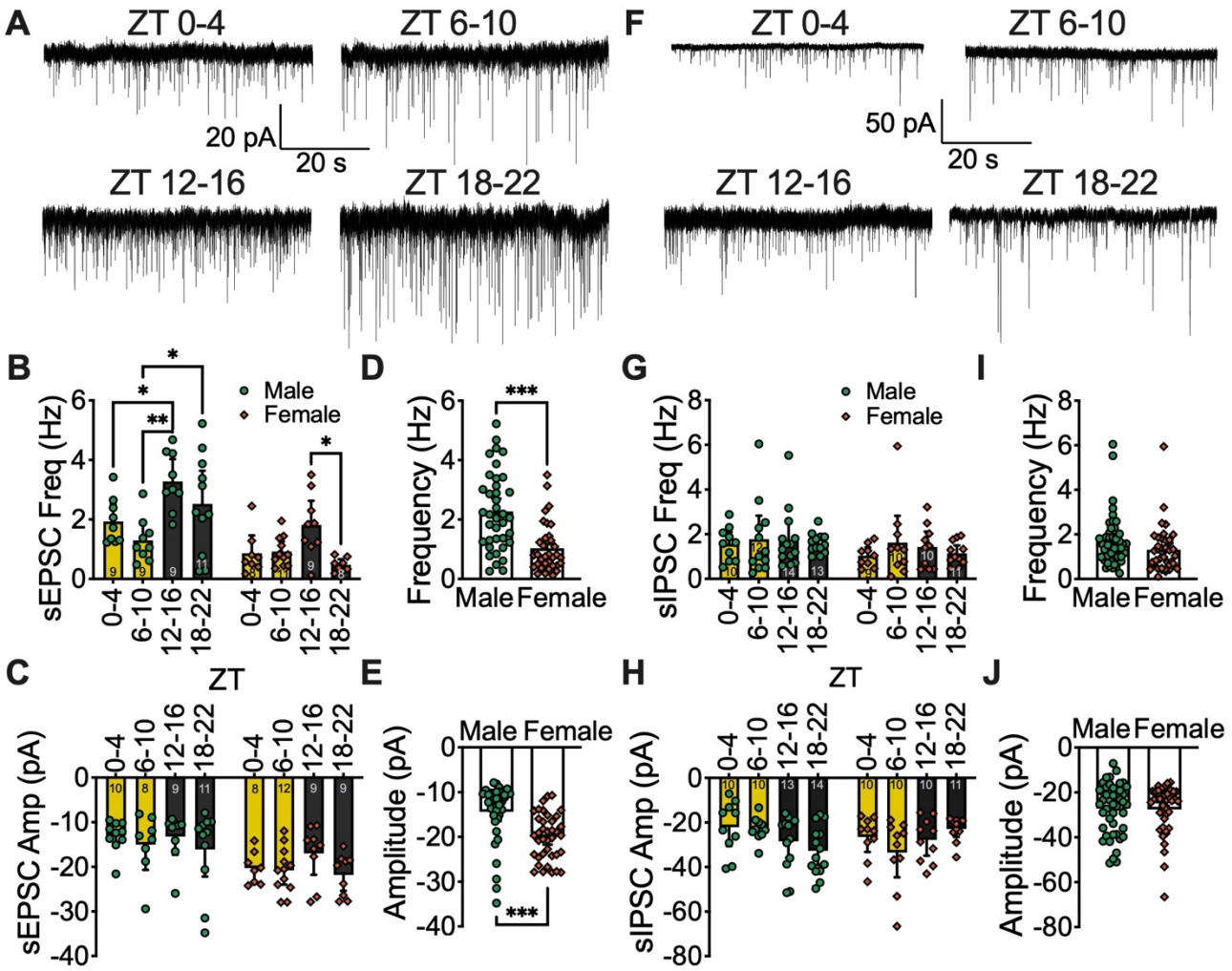

Figure 2. *Excitatory synaptic inputs onto plPFC pyramidal neurons are time-of-day dependent and differ by sex.* **(A)** Representative traces of sEPSC voltage clamp recordings from male mice at each ZT bin. **(B, D)** Mean and individual data points for sEPSC frequency and **(C, E)** amplitude at ZT0-4, 6-10, 12-16, and 18-22 or combined (*respectively*) in male (*bluish green circles*) and female (*vermillian diamonds*). **(F)** Representative traces of sIPSC voltage clamp recordings from male mice at each ZT bin. **(G, I)** Mean and individual data points for sIPSC frequency and **(H, J)** amplitude at ZT0-4, 6-10, 12-16, and 18-22 or combined (*respectively*) in male and female. Error bars represent ± 95%CI. N-values for number of cells inset on bars. Two-way ANOVA for main effects (including ***D, E, I and J***) and interaction, with a within group Tukey post-hoc analysis for ZT bin, *$p < 0.05$, **$p < 0.01$, ***$p < 0.001$. Exact p-values and analysis in **Figure 2 – source data 1**.

127 **Time-of-day does not alter sIPSCs in male or female mice**

128 Changes in RMP can be a consequence of intrinsic and/or synaptic properties. Our results on
129 sEPSC frequency and amplitude (**Figure 2A-E**) in the plPFC suggest that excitatory synaptic inputs are
130 not the primary driver of the daily changes in RMP illustrated in **Figure 1** and required further
131 investigation to identify the mechanism underlying time-of-day changes in resting state. To investigate
132 the contrast between daily changes in RMP and excitatory inputs, we predicted that if synaptic signaling
133 is a primary mediator of time-of-day changes in RMP then inhibitory inputs should be robust and
134 highest during the dark period ZT bins. GABAergic interneurons make up a small portion of PFC
135 neurons, but are highly involved in the regulation of pyramidal neurons and relay information between
136 different regions within the PFC (Saffari et al. 2016). To determine if inhibitory inputs contribute to the
137 diurnal tone of pyramidal neurons, we recorded (s) inhibitory postsynaptic currents (IPSCs; V_{Hold} = -
138 70mV) using a cesium chloride internal solution at ZT 0-4, 6-10, 12-16, and 18-22 (**Figure 2F-H**). We
139 did not observe a significant difference in sIPSC frequency or amplitude in male or female mice (**Figure**
140 **2F-J**), but noted a trend in increased amplitude during the dark period in male mice (**Figure 2F, H**).
141 Overall, these data do not support the notion that spontaneous synaptic inputs are the primary regulator
142 of daily rhythms in neuronal resting state in plPFC pyramidal neurons, suggesting that a postsynaptic
143 mechanism may regulate daily rhythms in these neurons.

144

145 **mIPSCs onto plPFC pyramidal neurons are time-of-day dependent**

146 Our central goal was to identify the mechanism(s) by which daily rhythms impact information
147 throughput of plPFC pyramidal neurons. Given that we did not observe daily changes of RMP in female
148 mice, and there was a main effect of sex on membrane resistance (**Figure 1C, E**), sEPSC frequency,
149 and amplitude (**Figure 2D, E**) – all without an interaction between sex and ZT bin – we proceeded with
150 our mechanistic investigation by separating male and females into independent groups.

151 Although we did not observe an effect of ZT bin on sIPSC frequency or amplitude in male mice,
152 when ZT bins were combined into light period and dark period, we uncovered a significant impact of the
153 LD cycle on sIPSC amplitude (**Figure 3B**). To further investigate whether time-of-day impacts the

154 presynaptic or postsynaptic components of inhibitory inputs, we measured mIPSCs by bath applying
155 the voltage-gated sodium channel blocker tetrodotoxin, which isolates the synapse from upstream
156 activity by inhibiting action potential firing. We observed no effect on mIPSC frequency, which is
157 typically associated with presynaptic neurotransmitter release, in male mice (**Figure 3A, C**). Although
158 we did not observe changes in decay tau or holding current, the time-of-day effect on IPSC amplitude
159 persisted in this configuration, and this increase in amplitude of inhibitory inputs is consistent with the
160 hyperpolarized RMP we observed during the dark period in male mice (**Figure 1C** and **3A, D-F**).
161 Notably, in female mice there was no LD effect on sIPSC amplitude (**Figure 3H**), but we did observe an
162 increase in mIPSC frequency and amplitude during the latter part of the light period (ZT 6-10; **Figure**
163 **3G, I-J**) although there was no effect on other potential postsynaptic measures, such as decay tau and
164 holding current (**Figure 3K, L**).
165

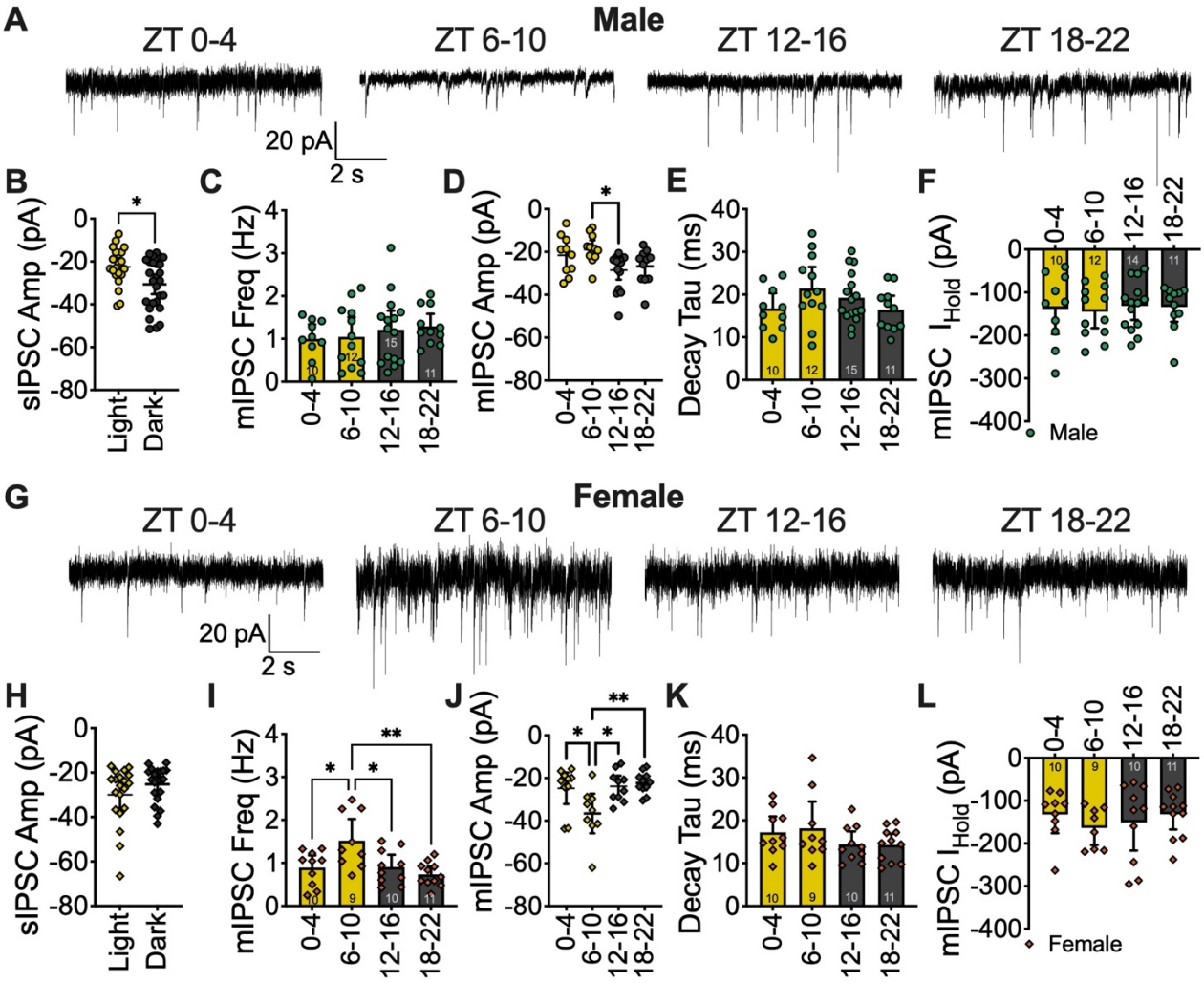

166

Figure 3. *Strength of inhibitory synaptic inputs onto plPFC pyramidal neurons are time-of-day dependent in male and female mice.* **(A)** Representative traces of mIPSC voltage clamp recordings from male and **(G)** female mice at each ZT bin. **(B, H)** Mean sIPSC amplitude in LD cycle (unpaired student t-test; yellow fill = light period, charcoal fill = dark period) and **(C, I)** mIPSC frequency, **(D, J)** amplitude, **(E, K)** decay tau, and **(F, L)** holding current (I_{Hold}) at ZT0-4, 6-10, 12-16, and 18-22 in male (*circles*) and female (*diamonds*) mice. Error bars represent ± 95%CI. One-way ANOVA with Tukey post-hoc analysis for ZT bin, *$p < 0.05$, **$p < 0.01$. N-values for number of cells inset on bars, exact p-values, mouse N-values, and analysis in **Figure 3 – source data 1**.

167 **Time-of-day impact on current voltage relationship in plPFC pyramidal neurons of female mice**

168 Although mIPSCs were enhanced during the latter portion of the light period (ZT6-10) in female
169 mice, we had not observed any convincing evidence of cell endogenous daily rhythms in the physiology
170 of plPFC pyramidal neurons in these mice. To investigate any potential daily changes in postsynaptic
171 properties we used a potassium (K^+) gluconate internal solution and measured the current-voltage (I-V)
172 relationship in these neurons by performing a voltage-step inactivation protocol in which neurons held
173 at -70mV were depolarized to 30mV and hyperpolarized in 10mV steps to a final MP of -120mV (**Figure**
174 **4A, B**). We analyzed the delayed steady-state current density (current density = (I_{Total})/(Cm)) during the
175 hyperpolarized (from -120 mV to -70mV (*K1*); **Figure 4A-C**) and depolarized state (0 mV to 30mV (*K2*);
176 **Figure 4A, B, E**), as well as daily changes in normalized conductance (g) calculated as the slope of the
177 K1 and K2 steady-state current normalized to cell capacitance: $g_{Normalized} = ((I_{VH2} – I_{VH1}) / (V_H2 –$
178 $V_H1))/(Cm)$, at different ZT bins (**Figure 4D, F**). We observed a main time-of-day effect on current
179 density and normalized conductance for the K1 hyperpolarized voltage steps, although there was no
180 main effect at the K2 depolarized voltage steps (**Figure 4B-F**). Together, these data demonstrate that
181 female mice do display daily rhythms in postsynaptic membrane properties, but they are not robust
182 enough to alter resting state (**Figure 1C-E**).
183

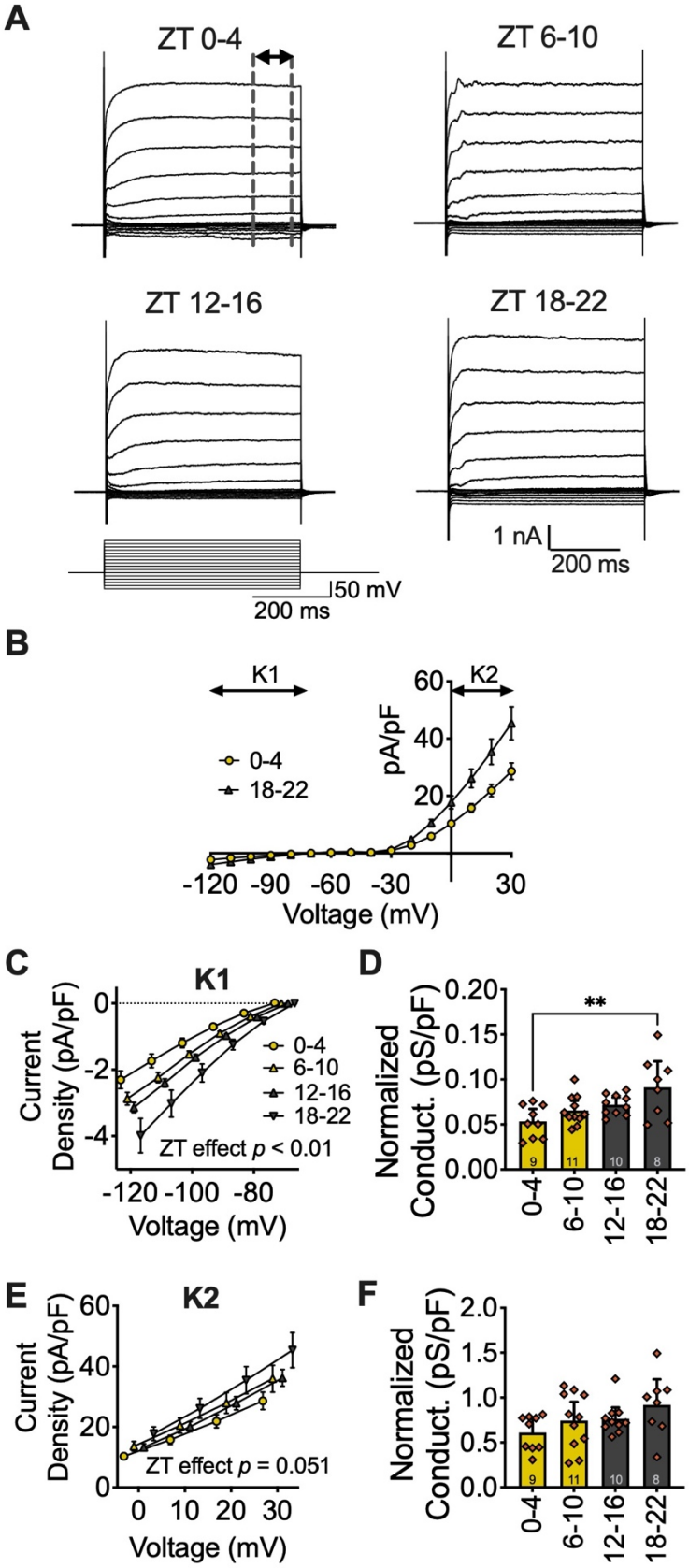
A
ZT 0-4
ZT 6-10
ZT 12-16
ZT 18-22
1 nA
200 ms
50 mV
200 ms
B
K1
K2
0-4
18-22
pA/pF
60
40
20
-120 -90 -60 -30 30
Voltage (mV)
C
K1
Current Density (pA/pF)
0
-2
-4
0-4
6-10
12-16
18-22
ZT effect p < 0.01
-120 -100 -80
Voltage (mV)
D
Normalized Conduct. (pS/pF)
0.20
0.15
0.10
0.05
0.00
**
9
11
10
8
0-4
6-10
12-16
18-22
E
K2
Current Density (pA/pF)
60
40
20
0
ZT effect p = 0.051
0 10 20 30
Voltage (mV)
F
Normalized Conduct. (pS/pF)
2.0
1.5
1.0
0.5
0.0
9
11
10
8
0-4
6-10
12-16
18-22

184

Figure 4. *Time-of-day impact on membrane conductance and currents in female mice.* **(A)** Current-voltage trace (*top; dashed line represents steady state current averaged for analysis*) after voltage-step protocol (*bottom*). **(B)** Averaged I-V voltage-step relationship from -120mV to 30mV for ZT0-4 and 18-22 (*normalized to cell capacitance*) with a K^+ internal solution. **(C, E)** Current density and **(D, F)** conductance of K1 and K2 currents (*respectively*) at ZT0-4, 6-10, 12-16, and 18-22 in female mice. K1 and K2 represent hyperpolarized and depolarized currents (*respectively*). Error bars represent ± 95%CI. Two-way (***C, E***) or One-way (***D, F***) ANOVA with Tukey post-hoc analysis for ZT bin. $^{**}p < 0.01$. N-values for number of cells inset on bars, exact p-values and analysis in **Figure 4 – source data 1**.

Time-of-day impact on current voltage relationship in plPFC pyramidal neurons of male mice

Given that synaptic inputs are rhythmic in male and female mice, but only male mice display daily rhythms in RMP, we hypothesized that changes in postsynaptic ionic currents, as measured by the I-V relationship, may play a role in setting the functional tone of plPFC pyramidal neurons in male mice. As in **Figure 4**, we analyzed the I-V relationship by running a voltage-step protocol (**Figure 5A, B**). In male mice the I-V relationship demonstrated a clear inward rectifying current at lower holding voltages and a delayed rectifying current at depolarizing voltages, resulting in a larger current density early in the dark period (ZT12-16) in both the hyperpolarized (**Figure 5A-C**) and depolarized state (**Figure 5A, B, D**). This effect translated into higher normalized cell conductance late in the light period and early in the dark period (**Figure 5I, J)**.

Since ionic conductance was highest at ZT12-16, the same ZT bin that RMP was most hyperpolarized, we predicted that this increase involved ion channel activity that results in a net negative current. Further, in the hyperpolarized state, the current density at each ZT began to converge near our calculated reversal potential for K^+. To determine if daily changes in current density and normalized cell conductance was dependent on K^+ channel activity, we utilized a K^+ free Cs^+-based internal recording solution to block outward K^+ currents. This preparation completely abolished the time-of-day effect on current density at lower holding voltages, but not in the depolarized state (**Figure 5E-**

203 **H**). Further, the time-of-day effect on normalized cell conductance was blocked when calculated at the
204 presented voltages with a main effect of Cs^+ on overall conductance in the depolarized state (**Figure**
205 **5I,J**). Of particular note, blockade of outward K^+ currents via internal Cs^+ appeared to have little effect
206 at ZT0-4, suggesting minimal K^+ channel activity at this ZT bin (**Figure 5C,G**). Together, these data
207 demonstrate that ion channel activity is time-of-day dependent in plPFC pyramidal neurons and K^+
208 channels contribute to daily rhythms in their cellular conductance.
209

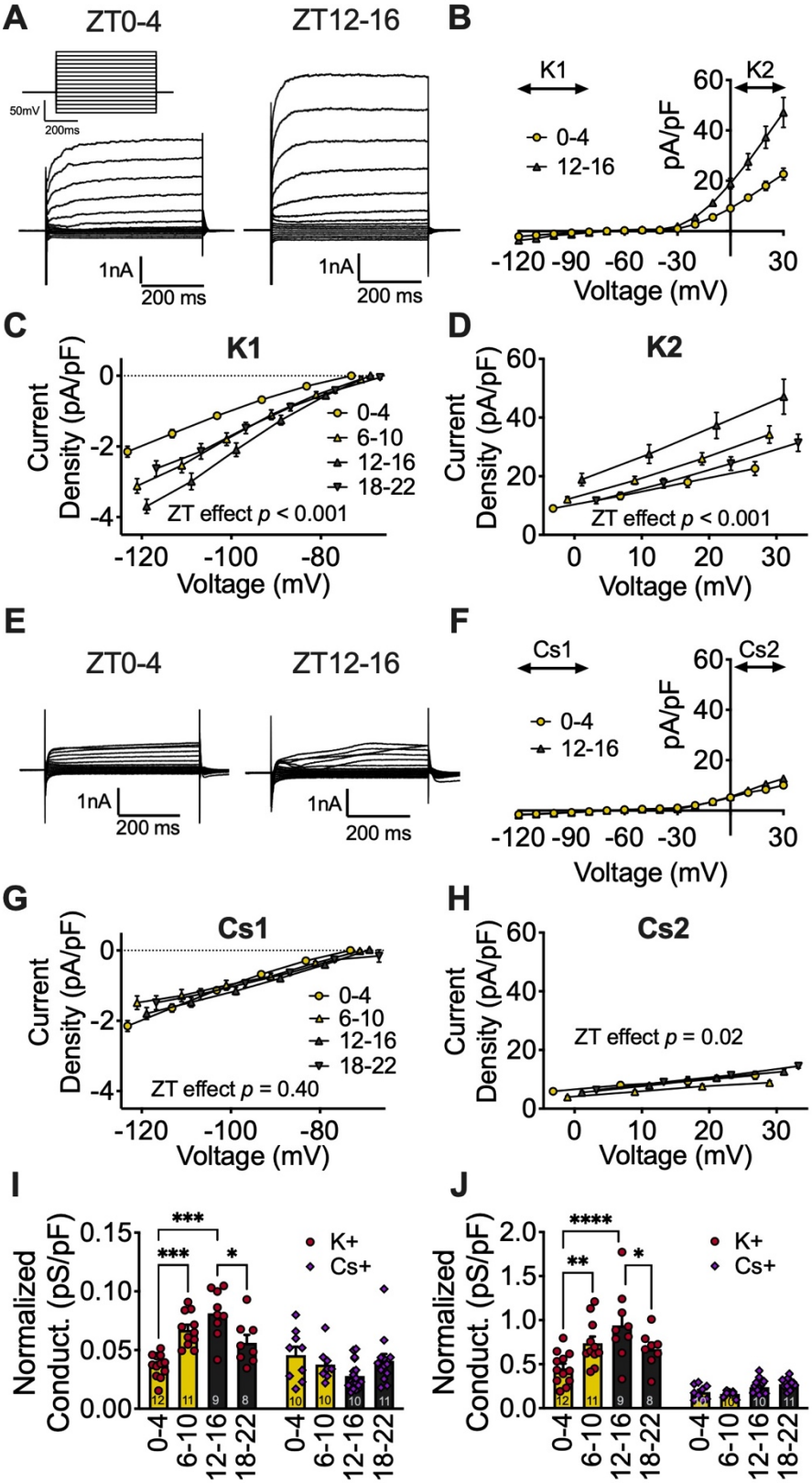
A
ZT0-4
ZT12-16
50mV
200ms
1nA
200 ms
B
K1
K2
0-4
12-16
pA/pF
Voltage (mV)
C
K1
Current Density (pA/pF)
0-4
6-10
12-16
18-22
ZT effect p < 0.001
Voltage (mV)
D
K2
ZT effect p < 0.001
E
F
Cs1
Cs2
G
Cs1
ZT effect p = 0.40
H
Cs2
ZT effect p = 0.02
I
Normalized Conduct. (pS/pF)
K+
Cs+
J

210

Figure 5. *Membrane conductances are mediated by K+ channels in males*

(A) Voltage-step protocol (*top left*) and representative voltage-step traces of I-V relationship at ZT 0-4 (*left*) and 12-16 (*right*) in male mice. **(B)** Averaged I-V relationship for ZT0-4 and 12-16 (*normalized to cell capacitance*) with a K^+ internal solution. **(C)** Current density of K1 and **(D)** K2 I-V relationships at ZT0-4, 6-10, 12-16, and 18-22. **(E)** Representative voltage-step traces of **(F)** I-V relationship at ZT 0-4 (*left*) and 12-16 (*right*) with a Cs+ internal solution. **(G)** Current density of Cs1 and **(H)** Cs2 I-V relationships at each ZT bin. **(I)** Comparison each ZT bin for K1 and Cs1, and **(J)** K2 and Cs2 normalized cell conductance. Two-way ANOVA for main effects and interaction, with a within group Tukey post-hoc analysis for ZT bin, voltage, and internal solution. Error bars represent ± 95%CI and N-values for recorded cells are inset in bars. *$p < 0.05$, **$p < 0.01$, ***$p < 0.001$. Exact p-values, mouse N-values, and analysis in **Figure 5 – source data 1**.

211
212 **Time-of-day alters excitability of plPFC pyramidal neurons**

213 To understand the functional implications of daily rhythms in RMP and postsynaptic ion channel
214 function for information throughput, we tested how time-of-day impacts action potential dynamics. We
215 utilized a 10 pA current injection protocol to evoke action potentials at ZT0-4, 6-10, 12-16, and 18-22
216 and observed a main effect of time for membrane potential threshold of action potential firing, with post-
217 hoc analysis revealing an increased threshold for firing late in the dark period (ZT18-22) when
218 compared to ZT6-10 in male mice (**Figure 6A-C**). Consistent with the null effect of time on RMP in
219 female mice, there was no effect of time on action potential threshold (**Figure 6C**). Further, although
220 there was no effect on amount of current needed to elicit an action potential (rheobase), once rheobase
221 was reached, subsequent current injections evoked action potential firing at a lower frequency during
222 the dark period (**Figure 6D, E**). Although we did not observe a time-of-day effect on action potential
223 amplitude or half-width in male mice (**Figure 6F-G**), decay tau was reduced at ZT18-22, a component
224 of action potential firing that is modulated to a large extent by K^+ channels (**Figure 6E**). These data
225 suggest that plPFC pyramidal neurons are not only more hyperpolarized during the light period, but are

226 functionally more difficult activate, requiring larger depolarizations to elicit action potentials and relay

227 information downstream.

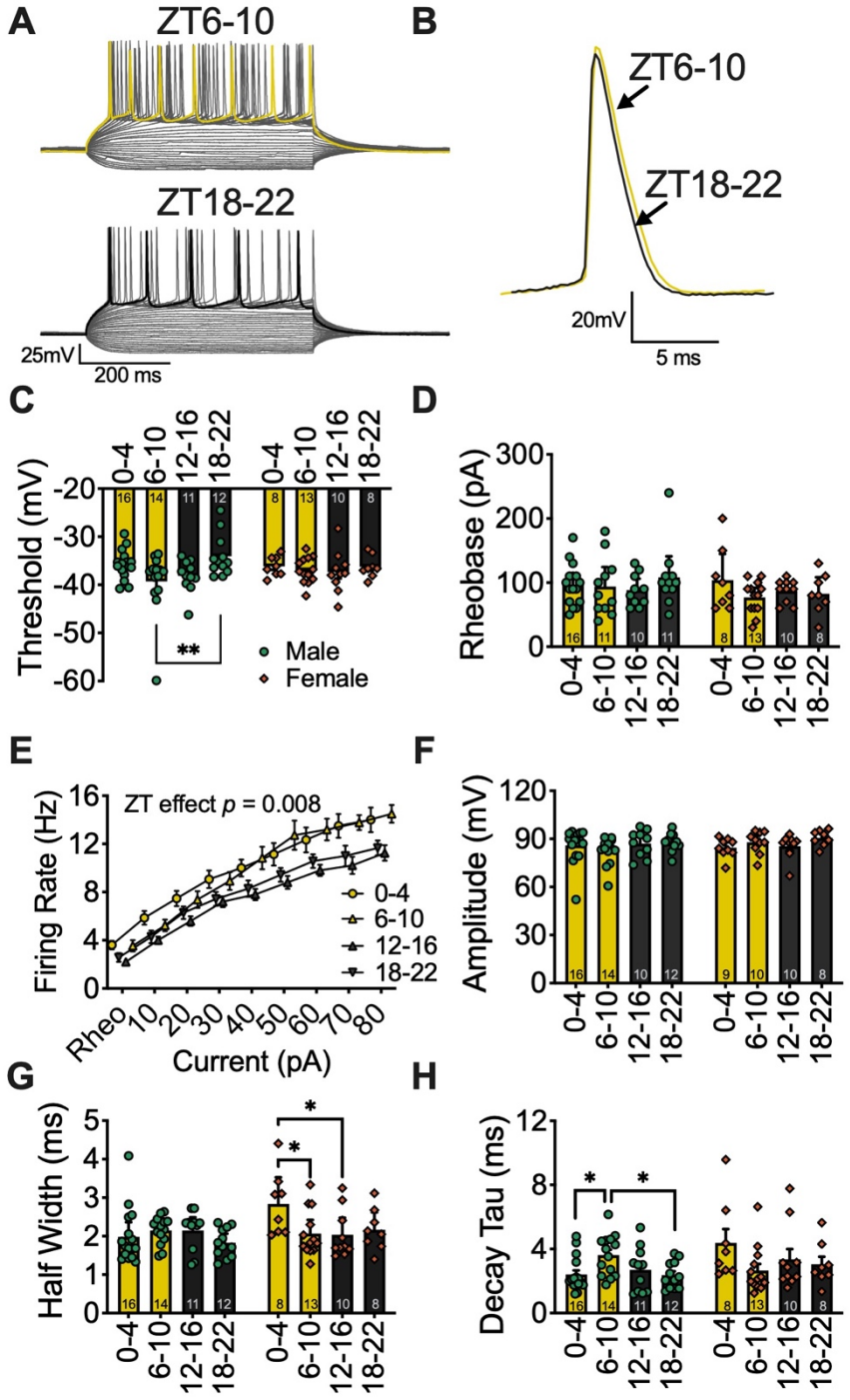

228

Figure 6. *Time-of-day differences in action potential dynamics.* **(A)** Representative trace of current step recording with maximal AP firing highlighted at ZT6-10 (*top; yellow*) and 18-22 (*bottom; black*) and **(B)** individual evoked APs in male mice. **(C)** Mean AP threshold **(D)** Rheobase, **(E)** evoked firing rate (from rheobase; male mice), **(F)** amplitude, **(G)** half width, and **(H)** decay tau at each ZT bin in male and female mice. Error bars represent ± 95%CI. Two-way ANOVA for main effects and interaction, with a within group Tukey post-hoc analysis for ZT bin and/or current injection. *$^{*}p < 0.05$, $^{**}p < 0.01$.* Number of cells included in for each bar. Exact p-values, mouse N-values, and analysis in **Figure 6 – source data 1**.

229

230 **Discussion**

231 The suprachiasmatic nucleus (SCN) is the central circadian clock in mammals and regulates
232 daily changes in gene expression and activity throughout the brain (M. H. Hastings, Reddy, and
233 Maywood 2003). However, it has become clear that numerous brain regions also display endogenous
234 daily rhythms. A major hypothesis in the field is that these extra-SCN clocks and the SCN operate
235 synergistically to drive daily rhythms in nearly all components of physiology and behavior, which is why
236 their disruption has numerous physiological and psychological consequences, including exacerbated
237 metabolic and mood disorders (Otsuka et al. 2020; McCarthy and Welsh 2012; Morris et al. 2015;
238 Bechtold, Gibbs, and Loudon 2010; Karatsoreos 2012). While there have been several well executed
239 studies that demonstrate the importance of circadian rhythms on neurophysiological function in the
240 hippocampus and brainstem, none have included the PFC, and all have largely focused on extracellular
241 field recordings (Chaudhury, Wang, and Colwell 2005; Loh et al. 2015; Paul et al. 2020; Chrobok et al.
242 2021; McMartin et al. 2021). Thus, previous studies have not shed light on the fundamental
243 electrophysiological processes at the cellular level that are affected by time-of-day.

244 In this study we present four main findings. First, layer 2/3 plPFC pyramidal neurons in male
245 mice are hyperpolarized during the early portion of the dark period when compared to the latter portion
246 of the light period. Second, time-of-day impacts excitatory and inhibitory inputs onto plPFC pyramidal
247 neurons, with clear sex differences in excitatory inputs. Third, we demonstrate that male mice display
248 distinct changes in ion channel activity and action potential kinetics, with male mice having an
249 increased action potential firing threshold and decreased decay tau during portions of the dark period.
250 Fourth, we identify that changes in K^+ channel activity serves as a potential mechanism underlying
251 time-of-day changes in the RMP and action potential firing rates of plPFC pyramidal neurons. By
252 identifying the intrinsic properties and synaptic inputs of plPFC pyramidal neurons, these findings allow
253 us to better understand the relationship between circadian rhythms, PFC circuitry and its associated
254 behaviors.

255 Changes in PFC function underly numerous psychiatric disorders including bipolar, post-
256 traumatic stress disorder (PTSD), attention deficit disorder, and deficits in learning and memory (Popoli

257 et al. 2012; Sotres-Bayon, Cain, and LeDoux 2006; Miller and Cohen 2001; Xu et al. 2019). There is
258 growing evidence of links between circadian rhythms and PFC function (Otsuka et al. 2020; Woodruff et
259 al. 2018; Hou et al. 2022; Harkness et al. 2021). Previous work from our group has demonstrated that
260 extracellular lactate (a functional output of neural metabolism) shows circadian rhythms in the medial
261 (m) PFC, and that environmental circadian disruption alters the morphology of medial mPFC neurons
262 and affects PFC mediated behaviors (Wallace et al. 2020; Karatsoreos et al. 2011). However, the
263 studies presented here are the first to explore whether cell autonomous activity and synaptic inputs
264 onto PFC neurons are rhythmic.

265 Our finding that the resting state of plPFC neurons is more hyperpolarized during the dark period,
266 when the animals are awake and active, suggests that these neurons are less active and require a
267 higher degree of information input before eliciting a response and sending downstream signals to other
268 brain regions. On the surface, it seems counter-intuitive that plPFC pyramidal neurons would be more
269 inactive during the dark period, when these animals are active and engaging with their environment,
270 than the light (inactive) period. A functional hypothesis for this finding is that stronger gating during the
271 wake period serves as a necessary mechanism for selective informational throughput in response to
272 environmental stimuli. Information filtering is paramount to having a proper behavioral output, and too
273 low of a threshold may result in overactivation as the animal engages with its environment. For
274 example, pharmacological studies have demonstrated that activation of the plPFC with neurotensin
275 agonists or the sodium channel activator veratrine lead to anxiogenic behaviors, likely through
276 increased glutamate release (Li, Chang, and Xi 2021; Petrie et al. 2004; Saitoh et al. 2014). Notably,
277 we discovered a large increase in excitatory inputs onto these neurons during the active period. This is
278 in line with other studies demonstrating that in layer 2/3 cortical neurons, excitatory inputs are
279 increased during spontaneous wakefulness and sleep deprivation occurring during the light (inactive)
280 period (Liu et al. 2010). While it seems contradictory that these neurons simultaneously receive more
281 excitatory inputs and become more hyperpolarized, it is aligned with the proposal that these neurons
282 require stronger gating mechanisms during the active period, as more information is being sent to these

283 neurons and it is critical that these incoming stimuli are somewhat filtered so only the strongest signals
284 are relayed further downstream.

285 Neurophysiological sex differences in the PFC, and their respective behavioral outputs, are well
286 documented and partly attributed to differences in synaptic signaling (Andrade et al. 2012; de Velasco
287 et al. 2015). While exploring the effects of time-of-day on these fundamental properties of PFC cells, we
288 fully embraced inclusion of both males and females, given the significant work demonstrating that
289 inclusion of both sexes (particularly inclusion of females) can reveal important new concepts and
290 understanding about brain function (Shansky and Murphy 2021). While not designed explicitly as a sex-
291 differences study, our results demonstrate that female mice had less excitatory inputs than males, yet
292 these inputs resulted in much larger postsynaptic currents, likely due to sex differences in glutamate
293 receptor expression and basal release (Perry et al. 2021). There are also sex differences in response to
294 environmental and pharmacological stressors, which are due in part to circulating sex hormones (Yuen,
295 Wei, and Yan 2016). For example, when compared to male rats, females in proestrus display a lower
296 threshold for impaired working memory after PFC injections of benzodiazepine inverse agonists that
297 activate the stress system, but this effect does not persist during estrus, when circulating estrogen
298 levels are lower (Shansky et al. 2004). Further, gonadal hormones underly sex differences in mPFC
299 dendritic growth, microglia activity, and astrocyte morphology in response to stress (Bollinger et al.
300 2019). It should be noted that there is a report that basal PFC glutamate release is higher in females,
301 which seems opposite to our findings, but is likely due to experimental differences, as these studies
302 differ in species, PFC layers, electrophysiological solutions, and time-of-day (Pena-Bravo et al. 2019).
303 We speculate that if the underlying mechanisms that mediate information throughput and plasticity are
304 fundamentally different in males and females, and the basal tone of excitatory inputs is relatively low in
305 females, then time-of-day changes in information filtering may not be as crucial to optimal plPFC
306 function in female mice.

307 GABAergic interneurons are highly involved in PFC function and relay information between
308 multiple regions of the PFC (Saffari et al. 2016; Hu, Gan, and Jonas 2014; Anderson et al. 2021). In the
309 hippocampus, GABAergic inputs onto CA1 pyramidal neurons regulate action potential firing frequency

310 in response to current injections, with a higher inhibitory tone during the light cycle (Fusilier et al. 2021;
311 Albers et al. 2017). Significantly, we found that in the plPFC there was no effect of sex or time-of-day
312 on spontaneous inhibitory inputs. This suggests that presynaptic inhibitory and excitatory inputs are not
313 the primary regulator of resting state or information throughput in layer 2/3 plPFC pyramidal neurons.
314 Instead, this supports the notion that basal inhibitory tone remains relatively constant throughout the
315 24h day and, in male mice, a postsynaptic cell endogenous mechanism is responsible for maintaining
316 proper information filtering when these neurons are challenged by the large increase of excitatory
317 signals that come in during the active period.

318 Although the frequency and amplitude of spontaneous inhibitory inputs did not change when
319 probed by individual ZT bins, further investigation revealed that when grouped by the light/dark cycle,
320 the strength (amplitude) of inhibitory inputs was stronger during the dark (active) period, specifically in
321 male mice. GABA receptors interact with postsynaptic ion channels and there are sex differences in the
322 expression of GABA receptor subunits, as well as how they interact with ion channels. For example, the
323 steroid hormone progesterone increases the expression of the $GABA_A$ receptor subunit α1 in the PFC
324 of rodents, and in humans, alcoholism is suggested to result in larger decreases of cortical GABA(A)
325 receptor subunits in females than males (Andrade et al. 2012; Janeczek et al. 2020). After investigating
326 GABAergic signaling localized at the synapse and isolated from upstream activity, we confirmed that
327 inhibitory postsynaptic currents are stronger early in the dark period in male mice. Interestingly, female
328 mice displayed a large increase in inhibitory inputs and strength late in the light period, a finding that
329 requires future studies to fully understand its functional implications.

330 In total, our findings point toward a postsynaptic mechanism underlying daily changes in the
331 physiology of layer 2/3 plPFC pyramidal neurons and previous work has shown that sleep deprivation
332 can alter the intrinsic excitability of layer 5 PFC pyramidal neurons (Yan et al. 2011). This prompted us
333 to explore how time-of-day impacts intrinsic postsynaptic properties such as ionic currents and overall
334 conductance. At hyperpolarized voltage steps below the reversal potential of K^+, time-of-day did have a
335 modest impact the conductance and current density of plPFC pyramidal neurons in female mice
336 between the transition from the dark to light period. However, at depolarizing voltages greater than the

337 mean RMP and action potential threshold there was no time-of-day effect. This further supports the
338 notion that while physiological daily rhythms do exist in plPFC pyramidal neurons of female mice, they
339 have little impact on overall resting state and information throughput in response to electrical activity
340 and synaptic inputs. In contrast, there was a large effect on the current density and conductance of
341 pyramidal neurons in male mice. Specifically, when these neurons were hyperpolarized below the
342 equilibrium potential for K^+, we discovered that current density increased throughout the light period,
343 peaking between the late period and early dark period. This effect translated into an overall increase in
344 conductance, and given that conductance was highest around the beginning of the active period, when
345 these neurons are most hyperpolarized, we presumed that this was due to an increased number of
346 open K^+ channels and the outflow of K^+ cations (outward current). Consistent with this prediction, when
347 we replaced K^+ with Cs^+ in our internal recording solution (to block K^+ channel mediated outward
348 currents), the time-of-day effect on current density and conductance was completely abolished at
349 voltages near or below the K^+ equilibrium potential. Although internal Cs^+ was not sufficient to block the
350 time-of-day effect on current density at depolarized voltage greater than the K^+ equilibrium potential, it
351 greatly reduced overall current density and conductance. Moreover, previous studies demonstrate that
352 internal Cs^+ is not sufficient to block the inward K^+ currents expected at voltages above the K^+
353 equilibrium potential (Adelman and Senft 1966).

354 To understand the functional relevance of these postsynaptic changes in ion channel function
355 and resting state, it was necessary to determine how time-of-day impacts action potential dynamics as
356 action potential firing is a functional measure for information throughput. Notably, this measure changes
357 with time-of-day in the hippocampus, and in response to sleep deprivation in the PFC (Fusilier et al.
358 2021; Yan et al. 2011). Action potentials are dependent on voltage-gated ion channels, and changes in
359 K^+ channel activity can alter action potential firing threshold and kinetics. Consistent with our
360 interpretation that, in male mice, there is a stronger gating mechanism to filter incoming signals during
361 the active period, we discovered that the threshold for action potential firing was increased during the
362 active period. These data suggest that layer 2/3 plPFC pyramidal neurons are not only more
363 hyperpolarized during the light period, but are functionally more difficult to activate, requiring much

364 larger depolarizations to elicit action potentials and relay information downstream. Though somewhat
365 speculative, this could affect a wide range of behaviors, including emotionality, a notion supported by
366 work demonstrating that pharmacological activation of plPFC neurons induces anxiogenic activity in
367 mice, and acute stress enhances glutamatergic transmission in the PFC (Yuen et al. 2009; Li, Chang,
368 and Xi 2021; Saitoh et al. 2014). Further, alcohol is a common drug of abuse in those suffering from
369 PFC associated affective pathologies, and in vivo electrophysiology studies show that alcohol preferring
370 rats have higher baseline neural firing in the PFC (Linsenbardt and Lapish 2015).
371 Combined, we believe this work demonstrates the importance of understanding how daily
372 rhythms impact neural function, which is necessary to fully grasp the relationships between brain and
373 behavior. It is critical to recognize that the mPFC is heterogeneous at the anatomical and physiological
374 levels, with consequences for behavior (Moorman et al. 2015). Our work suggests that even when
375 looking at the fundamental properties of cellular function in the mPFC, perhaps we need to add
376 heterogeneity at the temporal level as well. To fully appreciate the relationship between brain, behavior,
377 and daily rhythms, future studies are required to determine how these rhythms impact communication
378 with extra- (such as the hippocampus and amygdala) and intra- (such as the infralimbic) PFC regions.
379 Additionally, future studies are necessary to determine exactly which ion channels are mediating daily
380 changes in PFC function and how environmental factors that alter whole-animal physiology and
381 behavior, such as circadian disruption, may impact these circuits. Given the impact of time-of-day on
382 neuronal function in the PFC, the work presented here also has significant implications for incorporating
383 time-of-day into the application of pharmacological and behavioral interventions for mental health
384 disorders, and opens the door to similar questions in brain regions outside the PFC.
385

386 **Methods**

387 *Animals*

388 All animal procedures and experiments were approved by the University of Massachusetts
389 Amherst Institutional Care and Use Committee in accordance with the U.S. Public Health Service Policy
390 on Humane Care and Use of Laboratory Animals and the National Institutes of Health *Guide for the*
391 *Care and Use of Laboratory Animals*. Male and female wild-type mice (Charles River, Wilmington, MA,
392 USA) on a C57BL/6J background were used for these studies. All mice were group-housed in light
393 boxes at 25°C, under a 12/12-hr light/dark (LD) cycle, with food and water available *ad libitum*. Light
394 box LD cycles were offset so that experiments from each ZT bin occurred at the same time each day.
395 Mice ages 10-16 weeks were used for these studies. For electrophysiology studies mice were
396 anesthetized in a chamber with isoflurane before euthanasia by decapitation.

397

398 *Brain slice electrophysiology*

399 Two mice were simultaneously euthanized 1-hr prior to their ZT bin (i.e., mice were euthanized at
400 ZT23 for recording bin ZT0-4). After euthanasia, brains were immediately removed and the forebrain
401 was blocked while bathing in a 0-4°C oxygenated N-methyl-D-glucamine (NMDG) - 4-(2-hydroxyethyl)-
402 1-piperazineethanesulfonic acid (HEPES) cutting solution composed of (mM): 92 NMDG, 2.5 KCl, 1.25
403 NaH_2PO_4, 30 $NaHCO_3$, 3 sodium pyruvate, 2 thiourea, 20 HEPES, 10 $MgSO_4$, 0.5 $CaCl_2$, 25 glucose,
404 20 sucrose. Cutting solution was brought to pH 7.4 with ~17mL of 5M HCl (Ting et al. 2018). The
405 forebrains were mounted adjacent to each other and sectioned simultaneously on a vibratome
406 (VT1200S, Leica Biosciences, Buffalo Grove, IL, USA) with a sapphire knife (Delaware Diamond
407 Knives, Wilmington, DE, USA) yielding roughly three slices containing the PFC from each (250-μm) per
408 mouse. Slices were transferred and allowed to recover for 30-45 min in room temperature recording
409 artificial cerebrospinal fluid (aCSF) solution composed of (mM): 124 NaCl, 3.7 KCl, 2.6 NaH_2PO_4, 26
410 $NaHCO_3$, 2 $CaCl_2$, 2 $MgSO_4$, 10 glucose. aCSF had a final pH of 7.3-7.4, osmolarity of 307-310
411 mOsmos, and was continuously bubbled using 95% 0_2/5% $C0_2$. For recordings, brain slices were
412 transferred to a perfusion chamber containing aCSF maintained at 34-37°C with a flow rate of 1mL/min.

413 Neurons were visualized using an upright microscope (Zeiss Axoskop 2, Oberkochen, Germany).
414 Recording electrodes were back-filled with experiment-specific internal solutions as follows (mM):
415 Current-clamp and spontaneous (s) excitatory postsynaptic currents (EPSCs); 125 K-gluconate, 10
416 KCl, 10 NaCl, 5 HEPES, 10 EGTA, 1 $MgCl_2$, 3 NaATP and 0.25 NaGTP (liquid-junction potential (LJP)
417 = ~14.5 mV). Voltage-clamp spontaneous inhibitory postsynaptic currents (sIPSCs); 140 CsCl, 5 $MgCl_2$,
418 1 EGTA, 10 HEPES, 3 NaATP, and 0.25 NaGTP (LJP = ~4.2 mV). All internal solutions were brought to
419 pH 7.3 using KOH (current-clamp and EPSC) or CsOH (IPSC) at 301-304 mOsm. EPSCs were
420 recorded in the presence of the GABA receptor antagonist bicuculline (30 μM). sIPSCs were recorded
421 in the presence the competitive α-amino-3-hydroxy-5-methyl-4-isoxazolepropionic acid (AMPA)/kainate
422 receptor antagonist 6-cyano-7-nitroquinoxaline-2,3-dione (CNQX; 10 μM), the selective N-Methyl-d-
423 aspartate (NMDA) receptor antagonist (2R)-amino-5-phosphonovaleric acid (APV; 50 μM), and the
424 glycine antagonist strychnine (2 μM). Miniature (m) IPSCs had the addition of the voltage-gated sodium
425 channel (VGSC) blocker tetrodotoxin (TTX; 1 μM). Patch electrodes with a resistance of 3-5MΩ were
426 guided to neurons with an MPC-200-ROE controller and MP285 mechanical manipulator (Sutter
427 Instruments, Novato, CA, USA). Patch-clamp recordings were collected through a UPC-10 USB dual
428 digital amplifier and Patchmaster NEXT recording software (HEKA Elektronik GmbH, Reutlingen,
429 Germany). All voltage-clamp recordings were obtained at V_H= -70mV. Current clamp voltage-step
430 protocols were performed from the cell endogenous resting membrane potential, and used 500ms 10pA
431 steps from -100pA to +190pA. Voltage clamp current-step protocols were performed from V_H= -70mV,
432 and used 10mV steps from -120mV to +30mV. All compounds were obtained from Tocris Cookson,
433 Cayman Chemical, and Sigma Aldrich.
434 Individual recording locations were plotted (with neurons outside of the target area excluded
435 from analysis) as well as to qualitatively confirm an equal distribution of recording sites between
436 Zeitgeber (ZT) bins 0-4, 6-10, 12-16, and 18-22 (**Figure 1 – figure supplement 1A-D**). A small
437 percentage (~20%) of all recorded neurons had unique characteristics in resting membrane properties,
438 spontaneous excitatory postsynaptic currents (sEPSCs), and action potential dynamics that were
439 independent of time-of-day (hereafter Type II neurons; **Figure 1 - figure supplement 2A-I**). Most

notably, compared to Type I (most abundant) neurons, Type II neurons (less abundant) displayed a much higher action potential velocity and hyperpolarizing decay current (**Figure 1 - figure supplement 2A, B**). They also had a more depolarized resting membrane potential (RMP) and decreased action potential firing threshold (**Figure 1 - figure supplement 2E, F**). Due to these clear qualitative and quantitative differences independent of ZT bin, and that they represented a small proportion of recorded neurons, we excluded the far less abundant Type II neurons from analysis in our following experiments.

Statistical Analysis

For sEPSCs, only neurons with holding currents not exceeding 100pA at V_H= -70mV for the 10-min control period (input resistance > 70 MΩ) were studied further. Neurons were not considered for further analysis if series resistance exceeded 50MΩ or drifted >10% during baseline. Rheobase was calculated as the first current step to elicit an action potential and action potential dynamics (threshold, decay tau, and half-width) were obtained from the first evoked action potential to avoid variance in ion channel function due to repeated action potential firing. G*Power 3.0 software (Franz Faul, Uni Kiel, Germany) was used to conduct our power analysis, for a *p* value of <0.05 with 90% power. Adequate sample sizes were based upon expected effect sizes from similar experiments. Raw data files were analyzed in the Patchmaster NEXT software or converted using ABF Utility (Synaptosoft) for analysis in Clampfit (Molecular Devices, San Jose, CA, USA). N-values for analysis and presented in figures represent individual cells. To control for biological variability between groups N = 4-8 mice per group (see figure source data). Statistical comparison of effects between each time-period was made using a full model two-way ANOVA (column, row, and interaction effects) for comparison of the current-voltage relationships and comparing the interaction and main effect of time and sex or internal solution. For all experiments, error bars are presented as mean ± 95% confidence interval (CI). Statistics were calculated using Prism 9 (Graphpad Software, San Diego, CA, USA).

Acknowledgements

We would like to acknowledge and thank Dr. James Peters at Washington State University for his invaluable input and discussions during the preparation of this manuscript.

Grants

This work was supported by a CAREER grant 1553067 by the National Science Foundation, and R01 DK119811 from the National Institutes of Health to INK.

Competing Interests

BLR, JW and INK declare no competing financial interests.

476 **References**

477 Abe, Michikazu, Erik D. Herzog, Shin Yamazaki, Marty Straume, Hajime Tei, Yoshiyuki Sakaki,
478 Michael Menaker, and Gene D. Block. 2002. "Circadian Rhythms in Isolated Brain Regions."
479 *The Journal of Neuroscience* 22 (1): 350–56. https://doi.org/10.1523/JNEUROSCI.22-01-
480 00350.2002.

481 Adelman, W. J., and J. P. Senft. 1966. "Voltage Clamp Studies on the Effect of Internal Cesium Ion on
482 Sodium and Potassium Currents in the Squid Giant Axon." *The Journal of General Physiology*
483 50 (2): 279–93. https://doi.org/10.1085/jgp.50.2.279.

484 Aerde, Karlijn I. van, and Dirk Feldmeyer. 2015. "Morphological and Physiological Characterization of
485 Pyramidal Neuron Subtypes in Rat Medial Prefrontal Cortex." *Cerebral Cortex* 25 (3): 788–805.
486 https://doi.org/10.1093/cercor/bht278.

487 Albers, Elliott H., James C. Walton, Karen L. Gamble, John K. McNeill, and Daniel L. Hummer. 2017.
488 "The Dynamics of GABA Signaling: Revelations from the Circadian Pacemaker in the
489 Suprachiasmatic Nucleus." *Frontiers in Neuroendocrinology* 44 (January): 35–82.
490 https://doi.org/10.1016/j.yfrne.2016.11.003.

491 Albrecht, Anne, and Oliver Stork. 2017. "Circadian Rhythms in Fear Conditioning: An Overview of
492 Behavioral, Brain System, and Molecular Interactions." *Neural Plasticity* 2017: 3750307.
493 https://doi.org/10.1155/2017/3750307.

494 Anderson, Eden M., Skyler Demis, Hunter D'Acquisto, Annabel Engelhardt, and Matthew Hearing.
495 2021. "The Role of Parvalbumin Interneuron GIRK Signaling in the Regulation of Affect and
496 Cognition in Male and Female Mice." *Frontiers in Behavioral Neuroscience* 15 (March): 621751.
497 https://doi.org/10.3389/fnbeh.2021.621751.

498 Andrade, Susie, Bruno D. Arbo, Bruna A. M. Batista, Alice M. Neves, Gisele Branchini, Ilma S. Brum,
499 Helena M. T. Barros, Rosane Gomez, and Maria Flavia M. Ribeiro. 2012. "Effect of
500 Progesterone on the Expression of GABA(A) Receptor Subunits in the Prefrontal Cortex of
501 Rats: Implications of Sex Differences and Brain Hemisphere." *Cell Biochemistry and Function*
502 30 (8): 696–700. https://doi.org/10.1002/cbf.2854.

503 Bano-Otalora, Beatriz, Matthew J. Moye, Timothy Brown, Robert J. Lucas, Casey O. Diekman, and
504 Mino Dc Belle. 2021. “Daily Electrical Activity in the Master Circadian Clock of a Diurnal
505 Mammal.” *ELife* 10 (November): e68179. https://doi.org/10.7554/eLife.68179.
506 Bechtold, D. A., J. E. Gibbs, and A. S. Loudon. 2010. “Circadian Dysfunction in Disease.” *Trends*
507 *Pharmacol Sci* 31 (5): 191–98. https://doi.org/S0165-6147(10)00003-9 [pii]
508 10.1016/j.tips.2010.01.002.
509 Bollinger, Justin L., Isabella Salinas, Emily Fender, Dale R. Sengelaub, and Cara L. Wellman. 2019.
510 “Gonadal Hormones Differentially Regulate Sex-Specific Stress Effects on Glia in the Medial
511 Prefrontal Cortex.” *Journal of Neuroendocrinology* 31 (8): e12762.
512 https://doi.org/10.1111/jne.12762.
513 Chaudhury, D., L. M. Wang, and C. S. Colwell. 2005. “Circadian Regulation of Hippocampal Long-Term
514 Potentiation.” *J Biol Rhythms* 20 (3): 225–36. https://doi.org/20/3/225 [pii]
515 10.1177/0748730405276352.
516 Chrobok, Lukasz, Jasmin D. Klich, Jagoda S. Jeczmien-Lazur, Kamil Pradel, Katarzyna Palus-
517 Chramiec, Anna M. Sanetra, Hugh D. Piggins, and Marian H. Lewandowski. 2021. “Daily
518 Changes in Neuronal Activities of the Dorsal Motor Nucleus of the Vagus under Standard and
519 High-Fat Diet.” *The Journal of Physiology*, May. https://doi.org/10.1113/JP281596.
520 Chun, Lauren E., Elizabeth R. Woodruff, Sarah Morton, Laura R. Hinds, and Robert L. Spencer. 2015.
521 “Variations in Phase and Amplitude of Rhythmic Clock Gene Expression across Prefrontal
522 Cortex, Hippocampus, Amygdala, and Hypothalamic Paraventricular and Suprachiasmatic
523 Nuclei of Male and Female Rats.” *Journal of Biological Rhythms* 30 (5): 417–36.
524 https://doi.org/10.1177/0748730415598608.
525 Deng, Wei-Ke, Xing Wang, Hou-Cheng Zhou, and Fei Luo. 2019. “L-Type Ca2+ Channels and
526 Charybdotoxin-Sensitive Ca2+-Activated K+ Channels Are Required for Reduction of
527 GABAergic Activity Induced by B2-Adrenoceptor in the Prefrontal Cortex.” *Molecular and*
528 *Cellular Neurosciences* 101 (December): 103410. https://doi.org/10.1016/j.mcn.2019.103410.

529 Ferguson, Brielle R., and Wen-Jun Gao. 2018. “PV Interneurons: Critical Regulators of E/I Balance for
530 Prefrontal Cortex-Dependent Behavior and Psychiatric Disorders.” *Frontiers in Neural Circuits*
531 12. https://doi.org/10.3389/fncir.2018.00037.
532 Fusilier, Allison R., Jennifer A. Davis, Jodi R. Paul, Stefani D. Yates, Laura J. McMeekin, Lacy K.
533 Goode, Mugdha V. Mokashi, et al. 2021. “Dysregulated Clock Gene Expression and Abnormal
534 Diurnal Regulation of Hippocampal Inhibitory Transmission and Spatial Memory in Amyloid
535 Precursor Protein Transgenic Mice.” *Neurobiology of Disease* 158 (October): 105454.
536 https://doi.org/10.1016/j.nbd.2021.105454.
537 Harkness, John H., Angela E. Gonzalez, Priyanka N. Bushana, Emily T. Jorgensen, Deborah M.
538 Hegarty, Ariel A. Di Nardo, Alain Prochiantz, et al. 2021. “Diurnal Changes in Perineuronal Nets
539 and Parvalbumin Neurons in the Rat Medial Prefrontal Cortex.” *Brain Structure & Function* 226
540 (4): 1135–53. https://doi.org/10.1007/s00429-021-02229-4.
541 Hastings, J. W. 2007. “The Gonyaulax Clock at 50: Translational Control of Circadian Expression.” *Cold*
542 *Spring Harbor Symposia on Quantitative Biology* 72 (January): 141–44.
543 https://doi.org/10.1101/sqb.2007.72.026.
544 Hastings, Michael H., Akhilesh B. Reddy, and Elizabeth S. Maywood. 2003. “A Clockwork Web:
545 Circadian Timing in Brain and Periphery, in Health and Disease.” *Nature Reviews Neuroscience*
546 4 (8): 649–61. https://doi.org/10.1038/nrn1177.
547 Helm, Barbara, Rachel Ben-Shlomo, Michael J. Sheriff, Roelof A. Hut, Russell Foster, Brian M. Barnes,
548 and Davide Dominoni. 2013. “Annual Rhythms That Underlie Phenology: Biological Time-
549 Keeping Meets Environmental Change.” *Proceedings of the Royal Society B: Biological*
550 *Sciences* 280 (1765): 20130016. https://doi.org/10.1098/rspb.2013.0016.
551 Hou, YuanYuan, YunLei Wang, ShaoFei Song, Yao Zuo, HaoJie Zhang, Chen Bai, HaiTao Zhao, and
552 Tong Zhang. 2022. “Long-Term Variable Photoperiod Exposure Impairs the MPFC and Induces
553 Anxiety and Depression-like Behavior in Male Wistar Rats.” *Experimental Neurology* 347
554 (January): 113908. https://doi.org/10.1016/j.expneurol.2021.113908.

555 Hu, H., J. Gan, and P. Jonas. 2014. “Fast-Spiking, Parvalbumin+ GABAergic Interneurons: From
556 Cellular Design to Microcircuit Function.” *Science* 345 (6196): 1255263–1255263.
557 https://doi.org/10.1126/science.1255263.
558 Jagannath, Aarti, Lewis Taylor, Zeinab Wakaf, Sridhar R. Vasudevan, and Russell G. Foster. 2017.
559 “The Genetics of Circadian Rhythms, Sleep and Health.” *Human Molecular Genetics* 26 (R2):
560 R128–38. https://doi.org/10.1093/hmg/ddx240.
561 Janeczek, Paulina, Natalie Colson, Peter R. Dodd, and Joanne M. Lewohl. 2020. “Sex Differences in
562 the Expression of the A5 Subunit of the GABAA Receptor in Alcoholics with and without
563 Cirrhosis of the Liver.” *Alcoholism: Clinical and Experimental Research* 44 (2): 423–34.
564 https://doi.org/10.1111/acer.14266.
565 Kalmbach, Brian E., and Darrin H. Brager. 2020. “Fragile X Mental Retardation Protein Modulates
566 Somatic D-Type K+ Channels and Action Potential Threshold in the Mouse Prefrontal Cortex.”
567 *Journal of Neurophysiology* 124 (6): 1766–73. https://doi.org/10.1152/jn.00494.2020.
568 Karatsoreos, Ilia N. 2012. “Effects of Circadian Disruption on Mental and Physical Health.” *Curr Neurol*
569 *Neurosci Rep* 12 (2): 218–25. https://doi.org/10.1007/s11910-012-0252-0.
570 Karatsoreos, Ilia N., Sarah Bhagat, Erik B. Bloss, John H. Morrison, and Bruce S. McEwen. 2011.
571 “Disruption of Circadian Clocks Has Ramifications for Metabolism, Brain, and Behavior.”
572 *Proceedings of the National Academy of Sciences* 108 (4): 1657–62.
573 https://doi.org/10.1073/pnas.1018375108.
574 Kawaguchi, Y., and Y. Kubota. 1997. “GABAergic Cell Subtypes and Their Synaptic Connections in Rat
575 Frontal Cortex.” *Cerebral Cortex (New York, N.Y.: 1991)* 7 (6): 476–86.
576 https://doi.org/10.1093/cercor/7.6.476.
577 Körtner, Gerhard, and Fritz Geiser. 2000. “The Temporal Organization of Daily Torpor and Hibernation:
578 Circadian and Circannual Rhythms.” *Chronobiology International* 17 (2): 103–28.
579 https://doi.org/10.1081/cbi-100101036.
580 Landgraf, Dominic, Jaimie E. Long, Christophe D. Proulx, Rita Barandas, Roberto Malinow, and David
581 K. Welsh. 2016. “Genetic Disruption of Circadian Rhythms in the Suprachiasmatic Nucleus

582 Causes Helplessness, Behavioral Despair, and Anxiety-like Behavior in Mice." *Biological*
583 *Psychiatry* 80 (11): 827–35. https://doi.org/10.1016/j.biopsych.2016.03.1050.
584 Laroche, Serge, Therese M. Jay, and Anne-Marie Thierry. 1990. "Long-Term Potentiation in the
585 Prefrontal Cortex Following Stimulation of the Hippocampal CA1/Subicular Region."
586 *Neuroscience Letters* 114 (2): 184–90. https://doi.org/10.1016/0304-3940(90)90069-l.
587 Le Merre, Pierre, Sofie Ährlund-Richter, and Marie Carlén. 2021. "The Mouse Prefrontal Cortex: Unity
588 in Diversity." *Neuron* 109 (12): 1925–44. https://doi.org/10.1016/j.neuron.2021.03.035.
589 Li, Bin, Lei-Lei Chang, and Kang Xi. 2021. "Neurotensin 1 Receptor in the Prelimbic Cortex Regulates
590 Anxiety-like Behavior in Rats." *Progress in Neuro-Psychopharmacology and Biological*
591 *Psychiatry* 104 (January): 110011. https://doi.org/10.1016/j.pnpbp.2020.110011.
592 Linsenbardt, David N., and Christopher C. Lapish. 2015. "Neural Firing in the Prefrontal Cortex During
593 Alcohol Intake in Alcohol-Preferring 'P' Versus Wistar Rats." *Alcoholism, Clinical and*
594 *Experimental Research* 39 (9): 1642–53. https://doi.org/10.1111/acer.12804.
595 Liu, Zhong-Wu, Ugo Faraguna, Chiara Cirelli, Giulio Tononi, and Xiao-Bing Gao. 2010. "Direct
596 Evidence for Wake-Related Increases and Sleep-Related Decreases in Synaptic Strength in
597 Rodent Cortex." *Journal of Neuroscience* 30 (25): 8671–75.
598 https://doi.org/10.1523/JNEUROSCI.1409-10.2010.
599 Loh, Dawn H, Shekib A Jami, Richard E Flores, Danny Truong, Cristina A Ghiani, Thomas J O'Dell,
600 and Christopher S Colwell. 2015. "Misaligned Feeding Impairs Memories." Edited by Joseph S
601 Takahashi. *ELife* 4 (December): e09460. https://doi.org/10.7554/eLife.09460.
602 McCarthy, Michael J., and David K. Welsh. 2012. "Cellular Circadian Clocks in Mood Disorders:"
603 *Journal of Biological Rhythms*, September. https://doi.org/10.1177/0748730412456367.
604 McMartin, Laura, Marianna Kiraly, H. Craig Heller, Daniel V. Madison, and Norman F. Ruby. 2021.
605 "Disruption of Circadian Timing Increases Synaptic Inhibition and Reduces Cholinergic
606 Responsiveness in the Dentate Gyrus." *Hippocampus* 31 (4): 422–34.
607 https://doi.org/10.1002/hipo.23301.

608 Miller, Earl K., and Jonathan D. Cohen. 2001. “An Integrative Theory of Prefrontal Cortex Function.”
609 *Annual Review of Neuroscience* 24 (1): 167–202.
610 https://doi.org/10.1146/annurev.neuro.24.1.167.
611 Moorman, David E., Morgan H. James, Ellen M. McGlinchey, and Gary Aston-Jones. 2015. “Differential
612 Roles of Medial Prefrontal Subregions in the Regulation of Drug Seeking.” *Brain Research*, Role
613 of corticostriatal circuits in addiction, 1628 (December): 130–46.
614 https://doi.org/10.1016/j.brainres.2014.12.024.
615 Morris, C. J., J. N. Yang, J. I. Garcia, S. Myers, I. Bozzi, W. Wang, O. M. Buxton, S. A. Shea, and F. A.
616 Scheer. 2015. “Endogenous Circadian System and Circadian Misalignment Impact Glucose
617 Tolerance via Separate Mechanisms in Humans.” *Proc Natl Acad Sci U S A* 112 (17): E2225-
618 34. https://doi.org/10.1073/pnas.1418955112.
619 Otsuka, Tsuyoshi, Hue Thi Le, Akira Kohsaka, Fuyuki Sato, Hayato Ihara, Tomomi Nakao, and
620 Masanobu Maeda. 2020. “Adverse Effects of Circadian Disorganization on Mood and Molecular
621 Rhythms in the Prefrontal Cortex of Mice.” *Neuroscience* 432 (April): 44–54.
622 https://doi.org/10.1016/j.neuroscience.2020.02.013.
623 Paul, Jodi R., Jennifer A. Davis, Lacy K. Goode, Bryan K. Becker, Allison Fusilier, Aidan Meador-
624 Woodruff, and Karen L. Gamble. 2020. “Circadian Regulation of Membrane Physiology in
625 Neural Oscillators throughout the Brain.” *European Journal of Neuroscience* 51 (1): 109–38.
626 https://doi.org/10.1111/ejn.14343.
627 Pena-Bravo, Jose Ignacio, Rachel Penrod, Carmela M. Reichel, and Antonieta Lavin. 2019.
628 “Methamphetamine Self-Administration Elicits Sex-Related Changes in Postsynaptic Glutamate
629 Transmission in the Prefrontal Cortex.” *ENeuro* 6 (1): ENEURO.0401-18.2018.
630 https://doi.org/10.1523/ENEURO.0401-18.2018.
631 Perry, Christina J., Erin J. Campbell, Katherine D. Drummond, Jeremy S. Lum, and Jee Hyun Kim.
632 2021. “Sex Differences in the Neurochemistry of Frontal Cortex: Impact of Early Life Stress.”
633 *Journal of Neurochemistry* 157 (4): 963–81. https://doi.org/10.1111/jnc.15208.

634 Petrie, Kimberly A., Michael Bubser, Cheryl D. Casey, M. Duff Davis, Bryan L. Roth, and Ariel Y.
635 Deutch. 2004. “The Neurotensin Agonist PD149163 Increases Fos Expression in the Prefrontal
636 Cortex of the Rat.” *Neuropsychopharmacology* 29 (10): 1878–88.
637 https://doi.org/10.1038/sj.npp.1300494.
638 Piette, Charlotte, Marie Vandecasteele, Clémentine Bosch-Bouju, Valérie Goubard, Vincent Paillé,
639 Yihui Cui, Alexandre Mendes, et al. 2021. “Intracellular Properties of Deep-Layer Pyramidal
640 Neurons in Frontal Eye Field of Macaque Monkeys.” *Frontiers in Synaptic Neuroscience* 13:
641 725880. https://doi.org/10.3389/fnsyn.2021.725880.
642 Popoli, Maurizio, Zhen Yan, Bruce S. McEwen, and Gerard Sanacora. 2012. “The Stressed Synapse:
643 The Impact of Stress and Glucocorticoids on Glutamate Transmission.” *Nature Reviews*
644 *Neuroscience* 13 (1): 22–37. https://doi.org/10.1038/nrn3138.
645 Radnikow, Gabriele, and Dirk Feldmeyer. 2018. “Layer- and Cell Type-Specific Modulation of Excitatory
646 Neuronal Activity in the Neocortex.” *Frontiers in Neuroanatomy* 12.
647 https://doi.org/10.3389/fnana.2018.00001.
648 Saffari, R., Z. Teng, M. Zhang, M. Kravchenko, C. Hohoff, O. Ambrée, and W. Zhang. 2016. “NPY+-,
649 but Not PV+- GABAergic Neurons Mediated Long-Range Inhibition from Infra- to Prelimbic
650 Cortex.” *Translational Psychiatry* 6 (February): e736. https://doi.org/10.1038/tp.2016.7.
651 Saitoh, Akiyoshi, Masanori Ohashi, Satoshi Suzuki, Mai Tsukagoshi, Azusa Sugiyama, Misa Yamada,
652 Jun-Ichiro Oka, Masatoshi Inagaki, and Mitsuhiko Yamada. 2014. “Activation of the Prelimbic
653 Medial Prefrontal Cortex Induces Anxiety-like Behaviors via N-Methyl-D-Aspartate Receptor-
654 Mediated Glutamatergic Neurotransmission in Mice.” *Journal of Neuroscience Research* 92 (8):
655 1044–53. https://doi.org/10.1002/jnr.23391.
656 Sato, Keisaku, Fanyin Meng, Heather Francis, Nan Wu, Lixian Chen, Lindsey Kennedy, Tianhao Zhou,
657 et al. 2020. “Melatonin and Circadian Rhythms in Liver Diseases: Functional Roles and
658 Potential Therapies.” *Journal of Pineal Research* 68 (3): e12639.
659 https://doi.org/10.1111/jpi.12639.

660 Shansky, Rebecca M., C. Glavis-Bloom, D. Lerman, P. McRae, C. Benson, K. Miller, L. Cosand,
661 Thomas L. Horvath, and A. F. T. Arnsten. 2004. “Estrogen Mediates Sex Differences in Stress-
662 Induced Prefrontal Cortex Dysfunction.” *Molecular Psychiatry* 9 (5): 531–38.
663 https://doi.org/10.1038/sj.mp.4001435.
664 Shansky, Rebecca M., and Anne Z. Murphy. 2021. “Considering Sex as a Biological Variable Will
665 Require a Global Shift in Science Culture.” *Nature Neuroscience* 24 (4): 457–64.
666 https://doi.org/10.1038/s41593-021-00806-8.
667 Sotres-Bayon, Francisco, Christopher K. Cain, and Joseph E. LeDoux. 2006. “Brain Mechanisms of
668 Fear Extinction: Historical Perspectives on the Contribution of Prefrontal Cortex.” *Biological*
669 *Psychiatry* 60 (4): 329–36. https://doi.org/10.1016/j.biopsych.2005.10.012.
670 Ting, Jonathan T., Brian R. Lee, Peter Chong, Gilberto Soler-Llavina, Charles Cobbs, Christof Koch,
671 Hongkui Zeng, and Ed Lein. 2018. “Preparation of Acute Brain Slices Using an Optimized N-
672 Methyl-D-Glucamine Protective Recovery Method.” *JoVE (Journal of Visualized Experiments)*,
673 no. 132 (February): e53825. https://doi.org/10.3791/53825.
674 Velasco, Ezequiel Marron Fernandez de, Matthew Hearing, Zhilian Xia, Nicole C. Victoria, Rafael
675 Luján, and Kevin Wickman. 2015. “Sex Differences in GABABR-GIRK Signaling in Layer 5/6
676 Pyramidal Neurons of the Mouse Prelimbic Cortex.” *Neuropharmacology* 95 (August): 353–60.
677 https://doi.org/10.1016/j.neuropharm.2015.03.029.
678 Vertes, Robert P. 2006. “Interactions among the Medial Prefrontal Cortex, Hippocampus and Midline
679 Thalamus in Emotional and Cognitive Processing in the Rat.” *Neuroscience* 142 (1): 1–20.
680 https://doi.org/10.1016/j.neuroscience.2006.06.027.
681 Wallace, Naomi K., Felicity Pollard, Marina Savenkova, and Ilia N. Karatsoreos. 2020. “Effect of Aging
682 on Daily Rhythms of Lactate Metabolism in the Medial Prefrontal Cortex of Male Mice.”
683 *Neuroscience* 448 (November): 300–310. https://doi.org/10.1016/j.neuroscience.2020.07.032.
684 Weaver, David R. 1998. “The Suprachiasmatic Nucleus: A 25-Year Retrospective.” *Journal of Biological*
685 *Rhythms* 13 (2): 100–112. https://doi.org/10.1177/074873098128999952.

686 Woodruff, Elizabeth R., Lauren E. Chun, Laura R. Hinds, Nicholas M. Varra, Daniel Tirado, Sarah J.
687 Morton, Colleen A. McClung, and Robert L. Spencer. 2018. "Coordination between Prefrontal
688 Cortex Clock Gene Expression and Corticosterone Contributes to Enhanced Conditioned Fear
689 Extinction Recall." *ENeuro* 5 (6). https://doi.org/10.1523/ENEURO.0455-18.2018.
690 Workman, E. R., P. C. G. Haddick, K. Bush, G. A. Dilly, F. Niere, B. V. Zemelman, and K. F. Raab-
691 Graham. 2015. "Rapid Antidepressants Stimulate the Decoupling of GABA(B) Receptors from
692 GIRK/Kir3 Channels through Increased Protein Stability of 14-3-3η." *Molecular Psychiatry* 20
693 (3): 298–310. https://doi.org/10.1038/mp.2014.165.
694 Xu, Pan, Ai Chen, Yipeng Li, Xuezhi Xing, and Hui Lu. 2019. "Medial Prefrontal Cortex in Neurological
695 Diseases." *Physiological Genomics* 51 (9): 432–42.
696 https://doi.org/10.1152/physiolgenomics.00006.2019.
697 Yan, Jie, Jing-Cheng Li, Mei-Lan Xie, Dan Zhang, Ai-Ping Qi, Bo Hu, Wei Huang, Jian-Xia Xia, and Zhi-
698 An Hu. 2011. "Short-Term Sleep Deprivation Increases Intrinsic Excitability of Prefrontal Cortical
699 Neurons." *Brain Research* 1401 (July): 52–58. https://doi.org/10.1016/j.brainres.2011.05.032.
700 Yaniv, Yael, and Edward G. Lakatta. 2015. "The End Effector of Circadian Heart Rate Variation: The
701 Sinoatrial Node Pacemaker Cell." *BMB Reports* 48 (12): 677–84.
702 https://doi.org/10.5483/BMBRep.2015.48.12.061.
703 Yuen, Eunice Y., Wenhua Liu, Ilia N. Karatsoreos, Jian Feng, Bruce S. McEwen, and Zhen Yan. 2009.
704 "Acute Stress Enhances Glutamatergic Transmission in Prefrontal Cortex and Facilitates
705 Working Memory." *Proceedings of the National Academy of Sciences* 106 (33): 14075–79.
706 https://doi.org/10.1073/pnas.0906791106.
707 Yuen, Eunice Y., Jing Wei, and Zhen Yan. 2016. "Estrogen in Prefrontal Cortex Blocks Stress-Induced
708 Cognitive Impairments in Female Rats." *The Journal of Steroid Biochemistry and Molecular*
709 *Biology* 160 (June): 221–26. https://doi.org/10.1016/j.jsbmb.2015.08.028.
710 Zaitsev, A. V., N. V. Povysheva, G. Gonzalez-Burgos, and D. A. Lewis. 2012. "Electrophysiological
711 Classes of Layer 2/3 Pyramidal Cells in Monkey Prefrontal Cortex." *Journal of Neurophysiology*
712 108 (2): 595–609. https://doi.org/10.1152/jn.00859.2011.

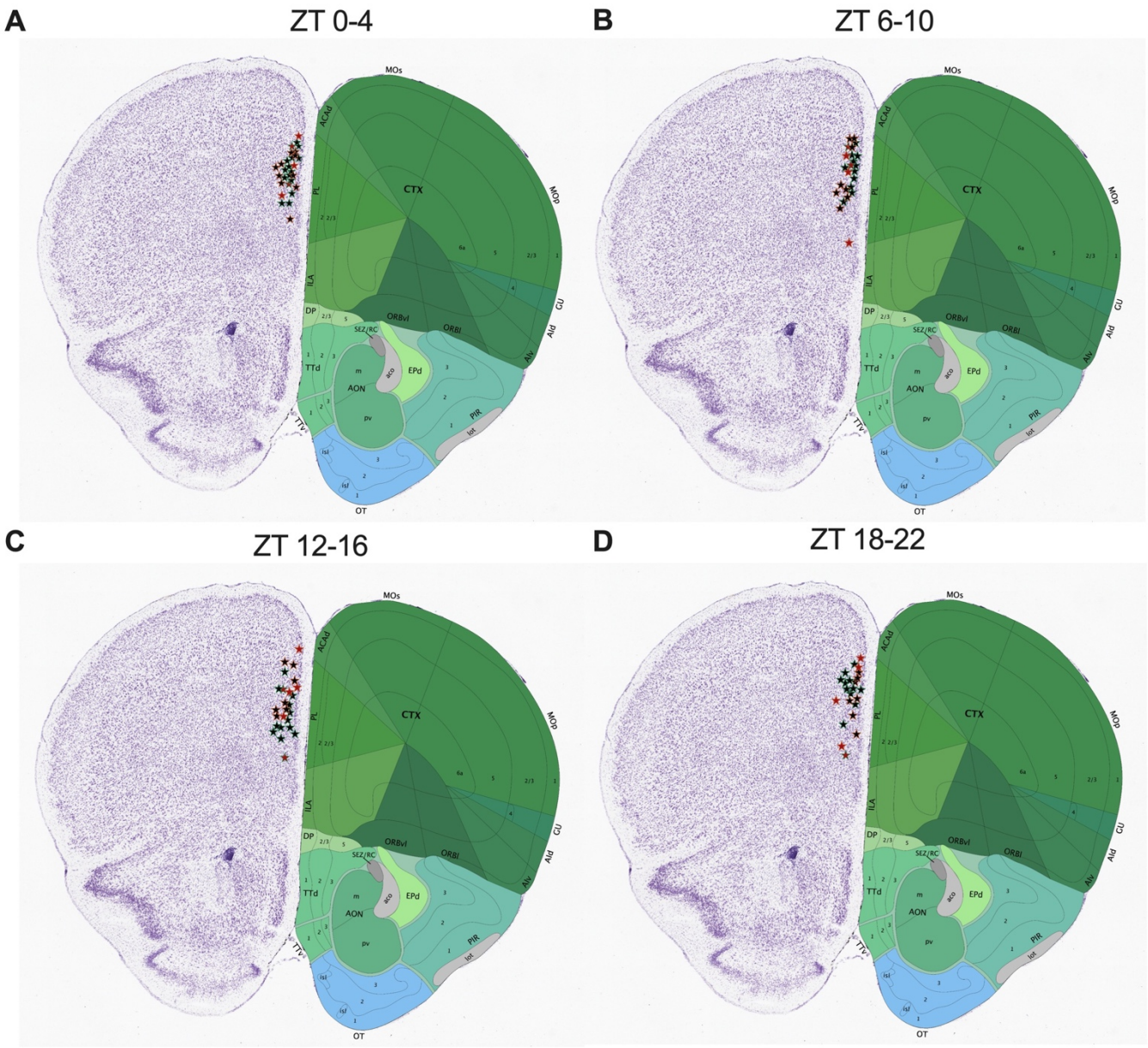

Figure 1 – figure supplement 1. *Recording map for layer 2/3 plPFC pyramidal neurons.* Coronal sections of forebrain showing individual recording sites from majority of neurons that were imaged at **(A)** ZT0-4, **(B)** 6-10, **(C)** 12-16 and **(D)** 18-22 for basal membrane property, sEPSC, and evoked action potential experiments in male (*bluish green outline*) and female (*vermillian outline*) mice. Stars filled with black represent 'Type I' neurons included for analysis and red stars represent Type II/III neurons excluded from analysis.

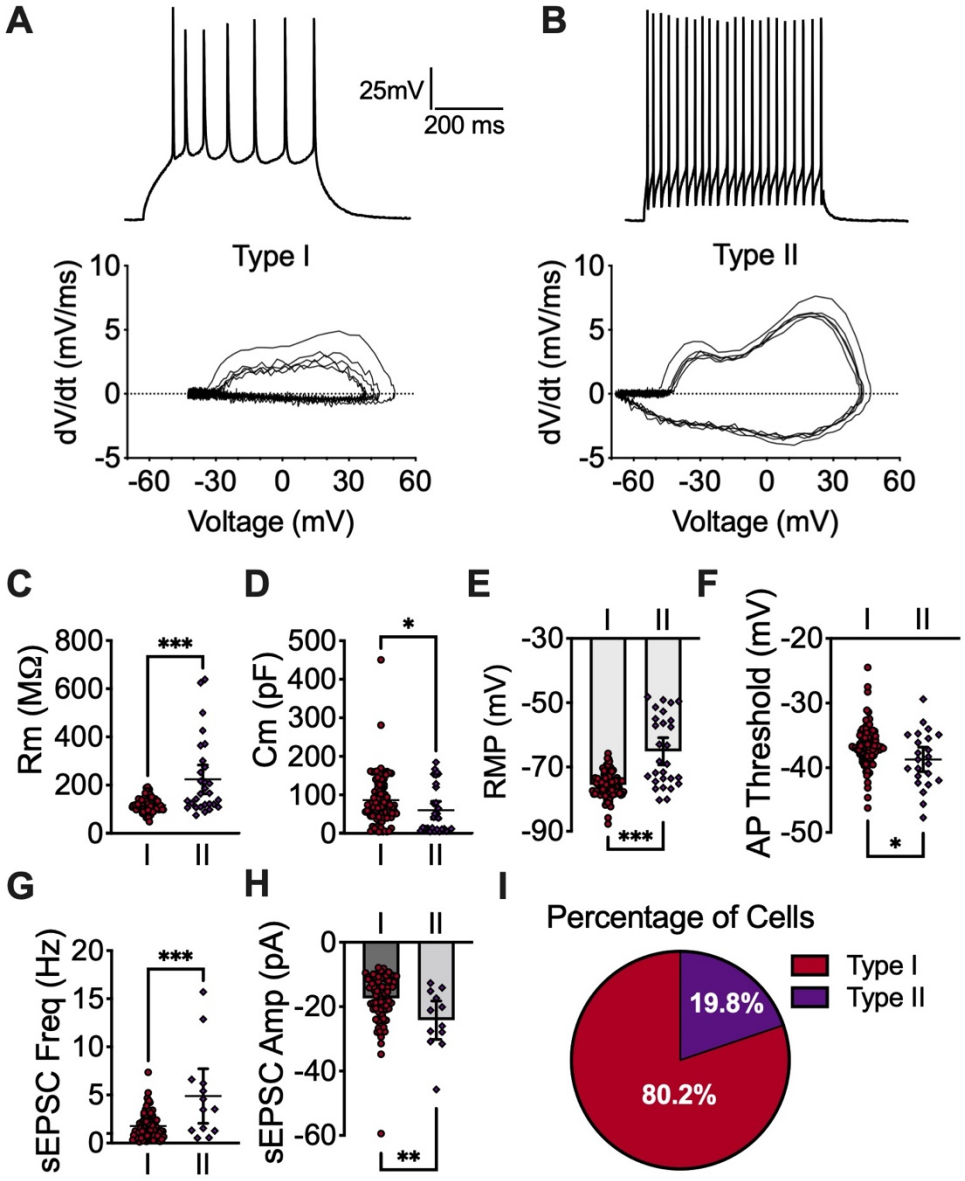

715

Figure 1 – figure supplement 2. *Categories and distinct physiological characteristics of plPFC neurons.* **(A)** Representative evoked action potential traces and phase plot diagram of first five action potentials (*bottom*) illustrating differences in velocity, trajectory, and amplitude in Type I and **(B)** Type II neurons. **(C)** Comparison of membrane resistance (Rm), **(D)** membrane capacitance (Cm), **(E)** resting membrane potential (RMP), **(F)** action potential (AP) threshold, **(G)** sEPSC frequency (Freq), and **(H)** sEPSC amplitude (Amp). **(I)** Percentage of recorded cells displaying Type I or Type II characteristics (combined among all ZT bins; calculated by *n* values from AP threshold). Error bars represent ± 95%CI. Unpaired student t-test, * $p< 0.05$, ** $p< 0.01$, *** $p< 0.001$. Exact p-values and analysis in **Figure 1 – supplemental source data 1**.